Local transport properties of thin bismuth films studied by scanning tunneling potentiometry

B. G. Briner* and R. M. Feenstra†

IBM Research Division, Thomas J. Watson Research Center, Yorktown Heights, New York 10598

T. P. Chin and J. M. Woodall

School of Electrical and Computer Engineering, Purdue University, West Lafayette, Indiana 47907

(Received 13 May 1996)

Charge transport in 20–30-Å-thick Bi films is studied by scanning tunneling potentiometry at room temperature. Deposition at $T = 140$ K onto InP-based multilayer substrates leads to flat and continuous films that are subjected to a lateral current density of up to 8×10^6 A/cm^2. We find that scattering at surface defects and grain boundaries gives rise to discontinuities in the local electrochemical potential. In particular, we observe dipole-shaped potential variations near small holes in the film. The influence of diffusive and ballistic transport on the formation of these dipoles is discussed. [S0163-1829(96)50832-5]

Charge transport in metals can be described from two complementary viewpoints. According to Ohm's law, the response of the metal to an externally applied field causes a current which is constant on a microscopic scale. The effective transport field experienced by the conduction electrons is averaged over the mean free path for electron-phonon scattering λ_{ep}. On the other hand, residual resistivity in a metal obviously is caused by scattering at localized deviations from the periodic lattice. It can't be expected that point defects or grain boundaries only give rise to current and field variations on a much larger scale. R. Landauer has emphasized the importance of this point, describing local transport fields as the response of the metal to the injected current. In a classical paper[1] he postulated the residual resistivity dipole (RRD) as elementary potential perturbation due to localized scattering. The Landauer theory was first considered as of rather academic value, because it does not predict different values for the metallic residual resistivity. With increasing interest in mesoscopic structures the RRD became fashionable with theorists, and today it is widely used as a starting point for descriptions of charge transport in low-dimensional conductors (see, e.g., Refs. 2–6). With the introduction of scanning tunneling potentiometry (STP) by Muralt et al.[7] an experimental technique for the possible observation of scattering-induced local-field variations became available. Kirtley et al. improved the STP sensitivity to the 10 μV level. These authors reported the observation of potential steps at grain boundaries of 600-Å-thick granular Au$_{60}$Pd$_{40}$ films, and interpreted these discontinuities as a result of strong localized scattering.[9] However, a subsequent study[10] seriously questioned their interpretation, and described the potential steps as artifacts caused by convolution of the STM tip with the substantial surface roughness of the investigated metal films. Recently, Besold et al.[11] obtained even better potential resolution, but their work on Au/C-films encountered the same tip-convolution problems that were addressed in Ref. 10.

Here we present a sample geometry to overcome the limitations imposed on STP by a rough surface. The cleaved (110) facet of an InP-based multilayer serves as an atomically flat template for the growth of thin ($d = 20$–30 Å) Bi

films. This sample geometry makes it possible to study charge transport with current densities up to $j = 8 \times 10^6$ A/cm^2, two orders of magnitude higher than the values reported in earlier studies.[9–12] The results unambiguously reveal the existence of potential discontinuities at surface holes and grain boundaries. A dipole-shaped potential feature is observed near strong scatterers. The very low carrier concentration of bulk Bi leads to a large mean free path, which would imply that ballistic effects have a dominant influence on the charge transport in the vicinity of surface defects. However, we find that the shape of the potential dipole closely resembles the result expected for diffusive transport. From this apparent discrepancy we infer that the mean free path in thin films is reduced because of an enhanced carrier density compared to bulk Bi. This confirms earlier studies[13] where it was shown that in the thin-film limit surface states dominate the DOS at the Fermi energy. Deviations between the experimental data and a computation for purely diffusive scattering provide evidence for the coexistence of ballistic and diffusive transport effects in the formation of the dipole.

A schematic layout of the sample geometry is shown in Fig. 1. Bi films are grown on a *n-i-n* semiconductor structure consisting of a semi-insulating spacer sandwiched between 500-nm-thick In$_{0.53}$Ga$_{0.47}$As layers, which are used to inject a lateral current (I_x) into the Bi film. Possible contact problems due to Schottky-barrier formation are avoided by the high dopant concentration ($n = 10^{19}$ cm^{-3}) in the injection layers. The spacer layer consists of either semi-insulating, Fe-doped InP or low-temperature grown, lightly *p*-doped In$_{0.52}$Al$_{0.48}$As. Substrate preparation, Bi evaporation, and subsequent potentiometry experiments are performed in the same UHV system with a base pressure of 4×10^{-11} Torr. After cleavage, the substrates are cooled down to 140 K. Bi (99.9999%) is evaporated out of a quartz crucible, at a rate of about 4 Å/min. Average film thicknesses are determined with a crystal deposition monitor. We find that cooling the substrates is necessary in order to obtain continuous and flat films. During Bi deposition the resistance across the sample starts to drop at a percolation thickness of only 6 Å, indicative of almost perfect film growth at $T = 140$ K. All potentiometry experiments are performed at room temperature.
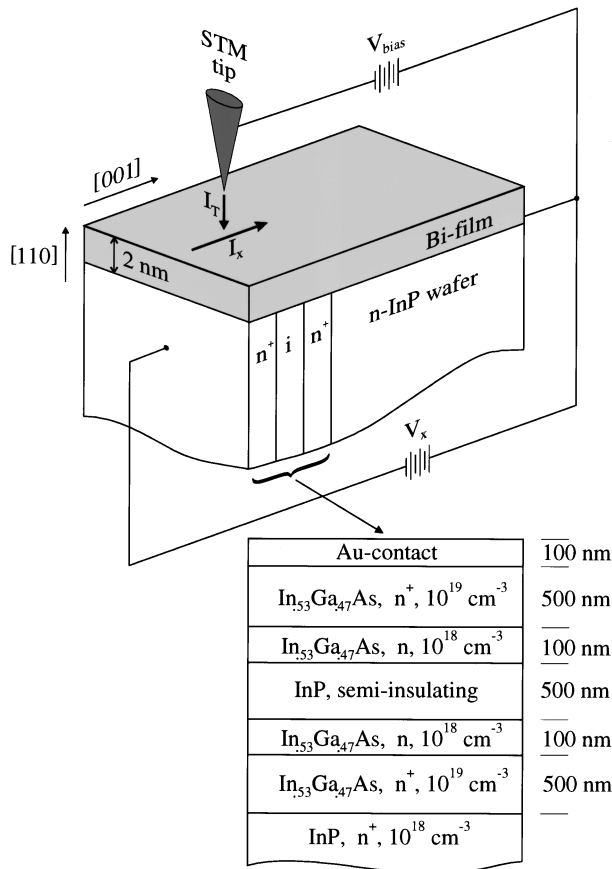
FIG. 1. Schematic drawing of the sample geometry, and cross section of InP-based multilayer used as substrate.
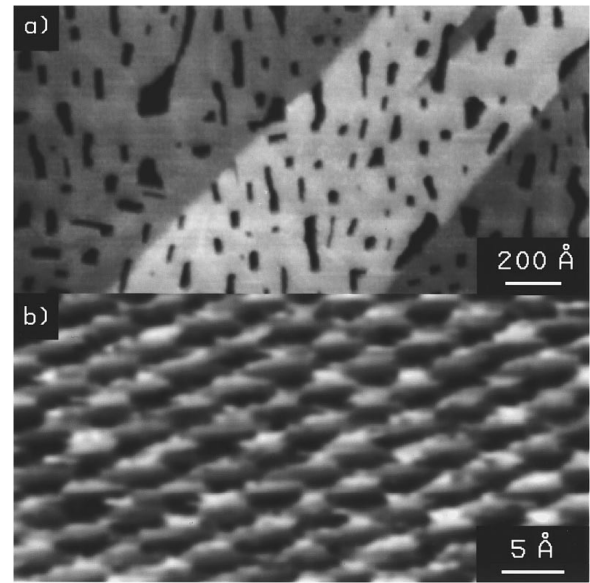

FIG. 2. STM topographs of a 25-Å-thick Bi film grown at $T = 140$ K onto the multilayer shown in Fig. 1. (a) Large-scale scan with atomically flat terraces and 12-Å-deep holes. (b) High-resolution image, not drift corrected. The close-packed structure of the Bi surface is visible.

From resistance measurements we infer that surface diffusion destroys the thinnest Bi films upon heating to $T = 300$ K. Therefore we always deposit at least 20-Å-thick overlayers for the present study. Figure 2(a) shows a 25-Å-thick Bi film after annealing to room temperature. The surface is characterized by atomically flat planes interspersed with irregularly shaped, 12-Å-deep holes.[14] A high-resolution image [Fig. 2(b)] reveals that the surface exhibits roughly hexagonal symmetry, i.e., Bi grows with the (111) direction of its pseudocubic unit cell perpendicular to the InP (110) plane. The 4-Å-high diagonal strip visible on Fig. 2(a) is a terrace on the substrate, a cleavage defect which is replicated in the overlayer. Room-temperature resistance of the Bi films typically lies between 3 and 5 Ω, corresponding to $\rho = 1 \times 10^{-3}$ Ω cm, about an order of magnitude larger than the bulk resistivity of Bi.

Potentiometry measurements are performed in a UHV STM with facilities for *in situ* sample and tip exchange, which has been described elsewhere.[15] Topography images are recorded with a constant tunneling current of 100 pA and a sample bias of 100–200 mV. To determine the local electrochemical potential V_0 we disable the STM feedback loop at each image pixel, and measure an *I-V* curve which typically extends over an interval of ± 50 mV around V_0. Usually, the tip-surface distance is slightly reduced after disabling the feedback in order to increase the current-detection sensitivity close to the zero-crossing point. V_0 is determined by interpolating the measured *I-V* data with a third-order

polynomial. We find that in our setup the sensitivity of the potential detection is currently limited to 0.5 mV by external noise sources. All investigated Bi films are good conductors, i.e., their *I-V* curves are almost linear close to V_0.

The potential distribution in a Bi film with 25 Å average thickness subject to a lateral current density of about 4×10^6 A/cm^2 is shown in Fig. 3(b) together with the simultaneously acquired topography image [Fig. 3(a)]. The potential image covers a range of 67 mV. It displays two distinct
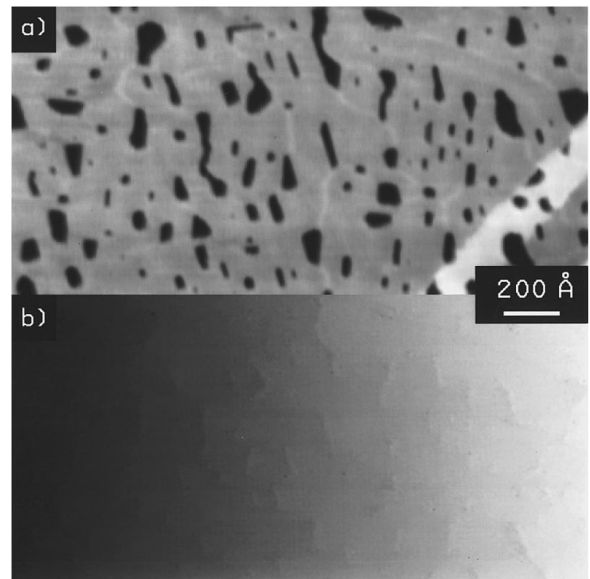

FIG. 3. Topography (a) and potential images (b), simultaneously recorded on a 30-Å-thick Bi film carrying a lateral current density of 4×10^6 A/cm^2. The gray-scale range in (b) corresponds to $\Delta V_0 = 67$ mV. Potential steps of 2–4 mV height appear at the sites of surface defects.
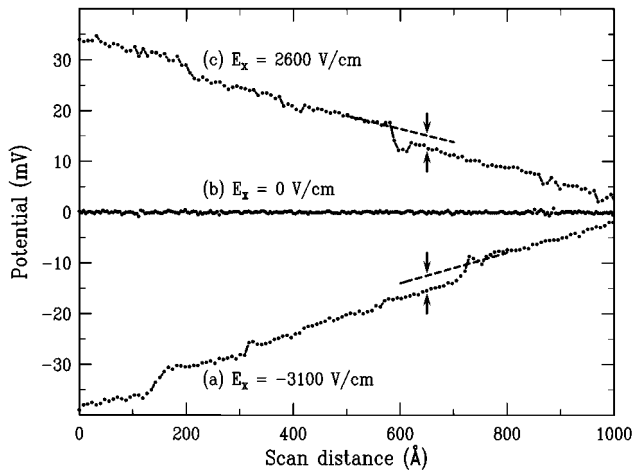
FIG. 4. Cross-sectional cuts of potential images on 25-Å-thick Bi films. Traces *a* and *c* are obtained with externally applied fields of -3100 V/cm and 2600 V/cm, trace *b* has been recorded without an external field. Potential steps on *a* and *c* are marked by arrows and dashed lines. The traces were acquired from different surface locations.

features which reflect the two different scattering mechanisms contributing to the resistivity of the Bi film. Phonon scattering is clearly manifest as a smooth ramp in the gray scale. However, in addition we find potential steps of 2–4 mV coinciding with the positions of the surface defects. These steps indicate that the 12-Å-deep holes act as localized scattering centers and significantly enhance the film resistivity. The faint lines visible in Fig. 3(a) are domain boundaries which extend from the holes and separate differently oriented areas of the Bi film. Close inspection reveals that these boundaries also give rise to small (≤ 1 mV) potential steps[16] (not visible in Fig. 3(b) because of the gray scale used). In Fig. 4 we present cross-sectional cuts of the potential distribution along the direction of the current flow. Trace *a* is extracted from Fig. 3(b) whereas trace *c* originates from a similar image with reversed in-plane current. On both curves the smooth potential ramp as well as the discontinuities at defect sites are discernible. Figure 4 proves that in our case the potential steps cannot be attributed merely to the tip-convolution effects which were met in earlier studies.[9–11] As indicated by the arrows in Fig. 4 the potential steps represent a real resistance increase—they lead to an offset between the flat parts of the potential curve. Tip convolution, on the other hand, would result in only a *single* potential ramp on flat portions of the film, interrupted by steps and terraces of $V_0 = $ const near strongly corrugated parts of the surface. A linecut taken from an image obtained without injecting any lateral current into the sample has been added to illustrate the sensitivity of our experimental setup (trace *b*).

We find that during prolonged current injection the Bi films undergo a strain relaxation process. As a consequence most of the 12-Å-deep holes disappear, and the surface now mainly consists of large terraces separated by 4- and 8-Å-high steps.[16] However, a few holes even increase in depth and become very dominant scatterers, which allow us to investigate the shape of the transport-induced potential distribution in more detail. Figure 5 shows how the local
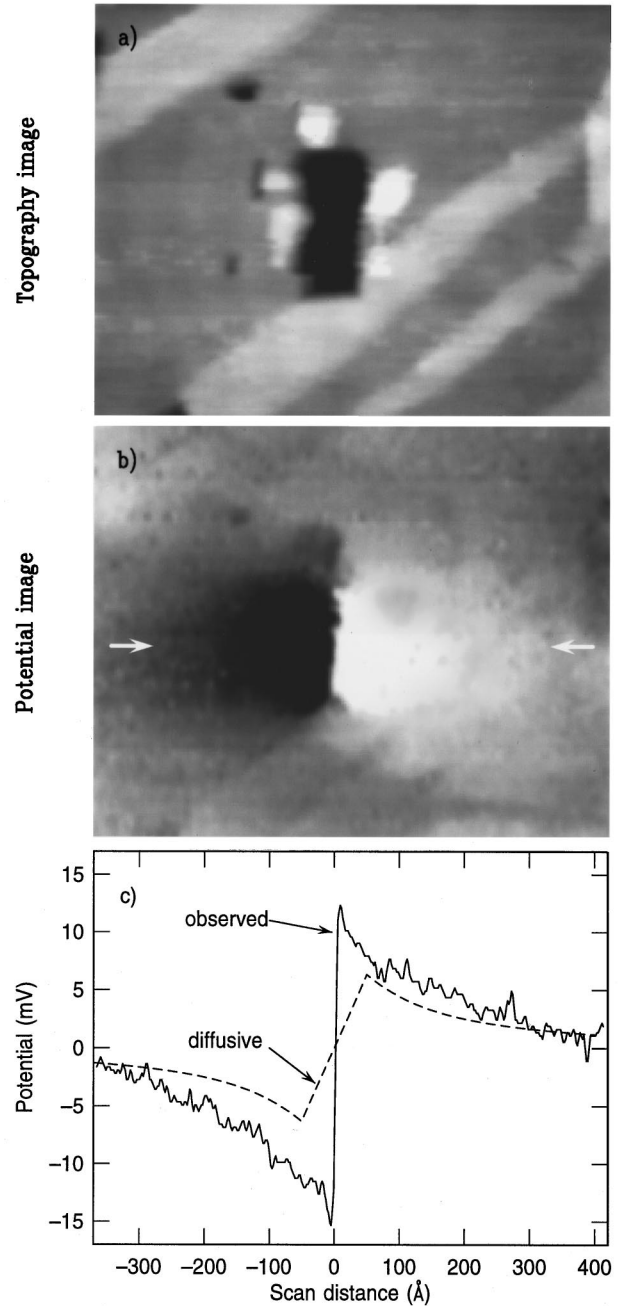

FIG. 5. (a) 640×800 Å^2 area of 30-Å-thick Bi film with a 24-Å-deep hole in the center. Pixel resolution = 3.5 Å. (b) Reduced STP potential after subtraction of a linear background. (c) Cross-sectional cut along the line marked by arrows in Fig. 5(b) (solid line), and computed curve for purely diffusive transport around the deep hole (dashed line). All three figures share the same *x*-axis calibration.

chemical potential is altered by scattering at one of the remaining surface defects. This image is observed on a Bi film with 30 Å average thickness carrying a current density of $\sim 4 \times 10^6$ A/cm^2. A 24-Å-deep hole located in the center of the topography image [Fig. 5(a)] gives rise to the surface potential presented in Fig. 5(b). A linear ramp ($E_x = 4400$ V/cm) has been subtracted from the STP image to highlight the part of the potential distribution which is induced by defect scattering. Figure 5(b) reveals a large dipole with its

lobes extending far beyond the topographical size of the surface defect. A horizontal linecut through the center of the dipole [Fig. 5(c)] illustrates the extension of the potential tails over several hundred Å.

To clarify the relative importance of diffusive (electron-phonon) and ballistic scattering for the formation of the dipole we calculate a model for purely diffusive transport around the deep hole by solving Ohm's law $\mathbf{J}=\sigma\mathbf{E}$ and $\nabla\cdot\mathbf{J}=0$ with the assumption that the hole extends completely through the Bi film. The shape of this ''diffusive'' dipole is represented by the dashed line in Fig. 5(c). Its magnitude is comparable to the STP data, indicating that electron-phonon scattering makes a dominant contribution to the defect-induced potential. From the qualitative agreement between experiment and the diffusive model we conclude that the mean free path $\lambda_{ep}=\sqrt{2m_{eff}E_F}/(ne^2\rho)$ must be smaller than the geometric size of the hole. With Ref. 17 and a surface-state density of $n_s=2.75\times10^{12}$ cm^{-2} (Ref. 13) we get $\lambda_{ep}=30$ Å. On the other hand, if we assume $n=n_{bulk}$,[17] the mean free path would be of the order of 1000 Å, much larger than the defect size. In the latter case the transport in the vicinity of the defect would be strongly influenced by ballistic processes analogous to those responsible for the formation of the RRD.[1,2,5]

Two differences are discernible between experiment and the diffusive model. In the interior of the hole the model yields a linear transition from negative to positive potential, whereas the experiment shows an abrupt transition at $d=0$ Å. This difference may not be significant, however, since tip-convolution effects *within* the hole could possibly produce such a sharp transition. More importantly, we find that the observed dipole is slightly larger than the computation, and there is a distinct asymmetry between the two dipole tails, with the left-hand lobe having about 20% more weight. A similar asymmetry has been observed on a number of the larger dipoles that we have studied. It has been theoretically demonstrated[5] that asymmetric dipoles occur for ballistic transport in the limit of high drift velocity. According to this theory the lobe on the ''downstream'' side of the defect becomes more pronounced as the drift velocity increases. For our case this effect would imply that in the sample depicted in Fig. 5 the current is carried mainly by holes. While in bulk Bi the electron and hole densities are about equal, Hoffmann *et al.*[13] have shown that the surface states are predominantly *p* type. This is a further indication that in our case the observed potential distribution is caused by scattering of surface states. Several theoretical papers have predicted that ballistic scattering leads to the formation of Friedel oscillations in the potential.[2–6] These oscillations rely on a sharp cutoff in the DOS at E_F, a condition which is not fulfilled in the present experiments since at 300 K the thermal energy k_BT is comparable to E_F in Bi. STP experiments at low temperature would offer a chance to see these oscillations, thus providing another view of possible ballistic effects in the transport.

---

*Present address: Fritz-Haber-Inst. der Max-Planck-Gesellschaft, Faradayweg 4-6, D-14195 Berlin, Germany. Electronic address: briner@fhi-berlin-mpg.de

†Present address: Department of Physics, Carnegie Mellon University, Pittsburgh, PA 15213. Electronic address: feenstra@andrew.cmu.edu

[1] R. Landauer, IBM J. Res. Dev. **1**, 223 (1957); R. Landauer, Z. Phys. B **21**, 247 (1975).

[2] R. S. Sorbello, Phys. Rev. B **23**, 5119 (1981); C. S. Chu and R. S. Sorbello, *ibid.* **40**, 5950 (1989).

[3] A. D. Stone and A. Szafer, IBM J. Res. Dev. **32**, 384 (1988).

[4] M. Büttiker, Phys. Rev. B **40**, 3409 (1989).

[5] W. Zwerger, L. Bönig, and K. Schönhammer, Phys. Rev. B **43**, 6434 (1991).

[6] M. Ya. Azbel', Phys. Rev. B **47**, 15 688 (1993).

[7] P. Muralt and D. Pohl, Appl. Phys. Lett. **48**, 514 (1986); P. Muralt, H. Meier, D. W. Pohl, and H. W. M. Salemink, *ibid.* **50**, 1352 (1987).

[8] G. Binnig, H. Rohrer, C. Gerber, and E. Weibel, Phys. Rev. Lett. **49**, 57 (1982).

[9] J. R. Kirtley, S. Washburn, and M. J. Brady, Phys. Rev. Lett. **60**, 1546 (1988).

[10] J. P. Pelz and R. H. Koch, Phys. Rev. B **41**, 1212 (1990).

[11] J. Besold, G. Reiss, and H. Hoffmann, Appl. Surf. Sci. **65/66**, 23 (1993).

[12] The current density in Ref. 9, p. 1548 should correctly read as $j=4\times10^4$ A/cm^2 [J. Kirtley (private communication)].

[13] C. A. Hoffmann *et al.*, Phys. Rev. B **48**, 11 431 (1993); Yu. F. Komnik *et al.*, Zh. Eksp. Teor. Fiz. **60**, 669 (1971) [Sov. Phys. JETP **33**, 364 (1971)].

[14] J. C. Patrin, Y. Z. Li, M. Chander, and J. H. Weaver, J. Vac. Sci. Technol. A **11**, 2073 (1993). These authors find a somewhat different morphology to that observed in the present work; we attribute this difference to different film thicknesses and annealing sequences.

[15] R. M. Feenstra, Phys. Rev. B **50**, 4561 (1994).

[16] B. G. Briner, R. M. Feenstra, T. P. Chin, and J. M. Woodall, Semicond. Sci. Technol. (to be published).

[17] $E_F=20$ meV, $m_{eff}=0.01$ m_0, $n_{bulk}=3\times10^{17}$ cm^{-3} electrons and holes.